

On the added benefits of ground-based LiDAR for wind turbine load measurements

M.J.S. Poodt
D.A.J. Wouters

January 2017
ECN-E--16-051



Acknowledgement

This report is written within “LiDAR Application for WINDfarm Efficiency” or LAWINE project partially funded by Dutch government under TKI Wind op Zee framework. The LAWINE project is coordinated by ECN, in cooperation with Delft University of Technology, Avent LiDAR Technology and XEMC Darwind. This body of work is carried out under subtask A of the LAWINE project (internal project number 5.2241).

‘Although the information contained in this report is derived from reliable sources and reasonable care has been taken in the compiling of this report, ECN cannot be held responsible by the user for any errors, inaccuracies and/or omissions contained therein, regardless of the cause, nor can ECN be held responsible for any damages that may result therefrom. Any use that is made of the information contained in this report and decisions made by the user on the basis of this information are for the account and risk of the user. In no event shall ECN, its managers, directors and/or employees have any liability for indirect, non-material or consequential damages, including loss of profit or revenue and loss of contracts or orders.’



Contents

	Summary	4
1	Introduction	5
2	Measurement campaign	7
2.1	EWTW Test Site	7
2.2	Meteorological mast 3	9
2.3	Ground based LiDAR	10
2.4	Wind turbine load measurements	11
2.5	Measurement data	12
3	Analysis of shear and loads	13
3.1	Introduction	13
3.2	Analysis of wind shear in measurement data	13
3.3	Effect of shear on Blade Out-of-plane Fatigue Moment	15
3.4	Effect of shear on Static Main shaft tilt moment	19
3.5	Effect of shear on Dynamic Main shaft fatigue bending moment	20
3.6	Effect of shear on Static Tower base for-aft bending moment	20
3.7	Effect of shear on Tower base for-aft fatigue bending moment	22
4	Conclusions & Recommendations	23
	References	25
	Appendices	
A.	Analysis of shear data	26

Summary

Within the project Lawine as part of Task A “Wind resource assessment“ an investigation has been made of the effect of the measured wind resource characteristics by means of LiDAR on the turbine behaviour in terms of mechanical loads. In particular the effect of vertical shear on turbine loads is investigated.

Measurement data from a campaign of 9 months on a 80m hub height turbine, a met mast and a ground based LiDAR were analysed. Distribution of shear in the data was analysed and shear exponent α in the dataset was found to be inversely correlated to turbulence intensity.

Turbine loads measurements for blades, main shaft and tower base were analysed. In the analysis the assumption that blade out-of-plane fatigue bending moment increases with higher shear was investigated. For low TI (0 to 4%) this assumption was confirmed. However for higher TI values the effect of turbulence dominates the blade out-of-plane fatigue load (15% higher out-of-plane EQL when TI increases from 2.5 to 17.5%).

Further observations were made on shear-dependency for blade, main shaft and tower loads. Main shaft average non-rotating bending moment was observed to increase with higher shear (i.e. up to 30% increase was observed). Average static tower base for-aft bending moment was observed to be independent from shear and is expected to be dominated by rotor thrust. Tower base for-aft fatigue equivalent bending moment however decreased with higher α (lower TI), similar to blade out-of-plane EQL.

Ground-based LiDAR measurements are concluded to provide a suitable method for refined determination of turbine loads.

1

Introduction

ECN has executed the project “LAWINE: LiDAR Application for WIND farmEfficiency” together with Delft University of Technology, Avent LiDAR Technology and XEMC Darwind in the framework of TKI Wind op Zee. The project is built around testing, evaluating and developing LiDAR technology.

In the LAWINE research project the following tasks are defined:

- Task A: Wind resource assessment
- Task B: Windscanner experiments
- Task C: Power performance using nacelle mounted LiDAR
- Task D: Nacelle mounted LiDAR assisted turbine control
- Task E: Wind farm optimization and wind farm control
- Task F: Efficiency improvement in LiDAR measurement campaign
- Task G: Development European research infrastructure ESFRI
- Task H: LiDAR calibration facility

The objective of Task A is to investigate:

- the accurate assessment of the local wind resource approaching the turbine measured by means of ground based LiDAR;
- the effect of the measured wind resource characteristics on the turbine behaviour in terms of mechanical loads and power production.

As part of Task A this report focusses on the mechanical loads assessment of a turbine using ground based LiDAR measurements. It describes the effect of one wind resource characteristic in particular: vertical shear. The topic of investigation is to what extent the ground based LiDAR provides an additional benefit compared to a traditional meteorological mast that is generally used in wind turbine load measurement campaigns, i.e. per IEC61400-13.

Chapter 2 describes the measurement campaign that was performed for task A. Based on an analysis of the collected measurement data the following questions are investigated In Chapter 3:

1. What distribution of vertical wind shear is contained in the measurements?
2. What load quantities of the turbine show a dependence on vertical wind shear?

3. Does a ground-based LiDAR provide a benefit compared to a meteorological mast when measuring the effect of vertical shear on wind turbine loads?

2

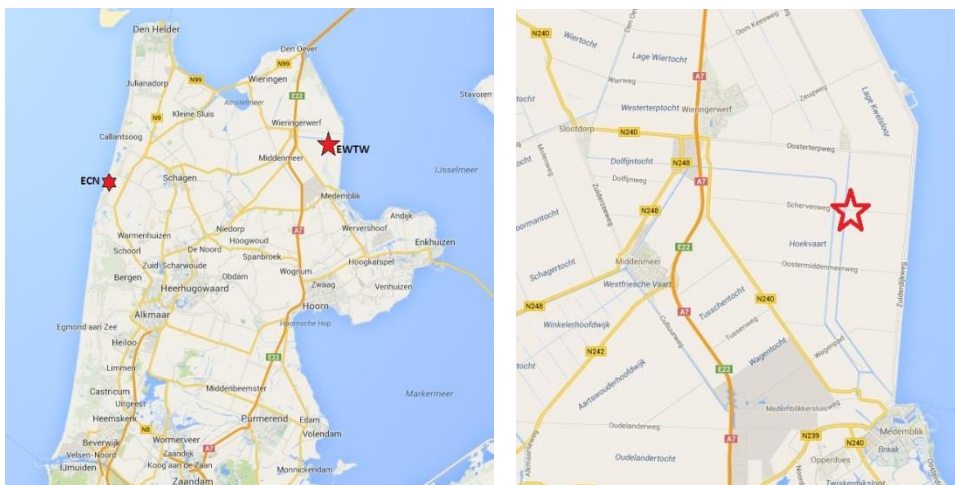
Measurement campaign

This chapter summarizes the most relevant information of the ECN Wind turbine Test site Wieringermeer (EWTW) and the mechanical load measurement campaign performed for the project. More detailed information of the test site and the instrumentation of the meteorological mast 3 (MM3) and the ground-based LiDAR can be found in [2].

2.1 EWTW Test Site

The ECN Wind turbine Test site Wieringermeer is located in the polder Wieringermeer, in the North East of the Province Noord-Holland of the Netherlands, 27 km East of ECN Petten (see **Figure 1**).

Figure 1: Map of the province Noord-Holland (left) and a detailed map of the test site EWTW (right).



The test site and its surroundings are characterised by flat terrain, consisting of mainly agricultural area with single farmhouses and rows of trees. The lake IJsselmeer is located at a distance of 2 km East of meteorological mast 3 (MM3). The location of MM3, the ground based LiDAR and the wind turbines at EWTW are shown in **Figure 2**. Research turbine number 6 is used in this project.

Figure 2: Layout of the test site EWTW: the meteorological mast 3 is surrounded by 5 research turbines (WT5 – WT9), 6 prototype wind turbines (WT1 –WT 4,WT 10,WT 11) and 4 smaller single wind turbines. The location of the ground based LiDAR is denoted by the black square south of the meteorological mast 3.



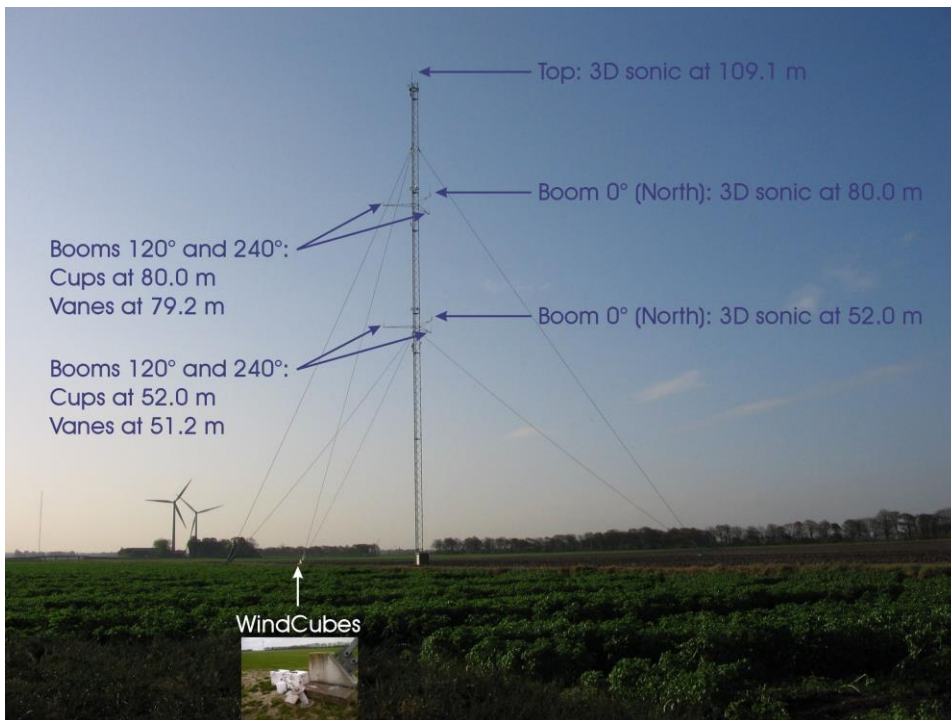
2.2 Meteorological mast 3

The meteorological mast 3 (MM3) is located approximately 200 m south of a line of 5 research wind turbines of 2.5MW, see **Figure 2**. About 1,5 km south of the met mast a line of 6 large prototype wind turbines is located. Within the same distance, also 4 smaller wind turbines are operating.

On two booms pointing north (0°) at 52.0 and 80.0 m height 3D sonic anemometers (Gill) are mounted. Both at 50.4 and 78.4 m height two booms (120° and 240°) are mounted with cup anemometers (52.0 and 80 m height) and wind vanes (51.2 and 79.2 m height).

On top of the mast a sonic anemometer is mounted on the East pillar at 109.1 m height. This anemometer is undisturbed by the mast except for the wind direction of 210° at which the top anemometer is in the wake of the lightning rod mounted on the South pillar.

Figure 3: Relevant signals of meteorological mast 3. Photograph taken from the tower base of research turbine 6, see also **Figure 2**.



2.3 Ground based LiDAR

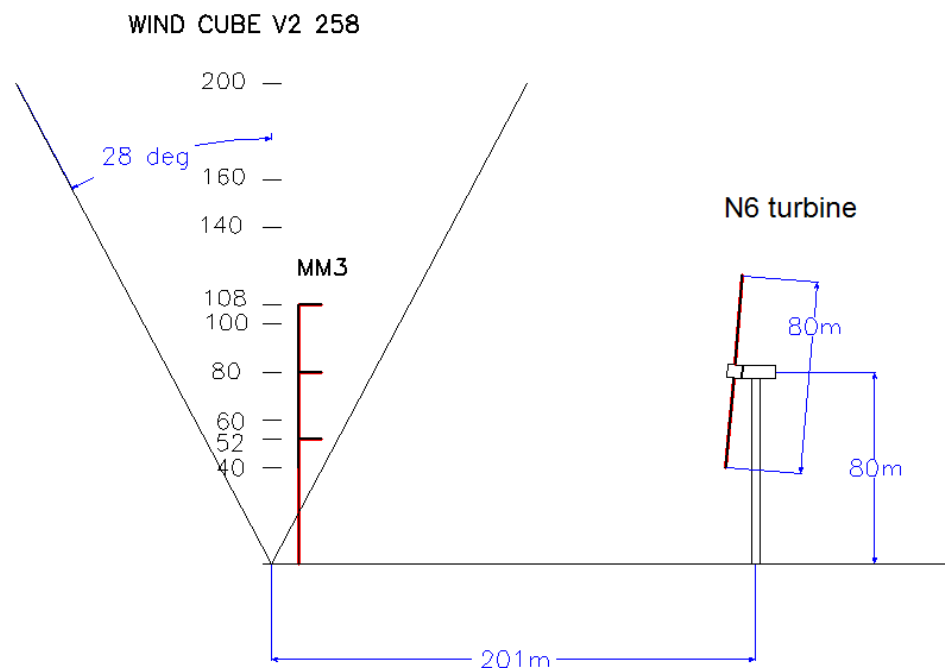
The WindCubeV2 is a ground based LiDAR (Light Detection And Ranging) system that sends infrared laser pulses into the atmosphere, using four beams along a 28° cone angle. The wind speed is determined from the Doppler shift of the backscattered light.

The WindCubeV2 system (WC258) is located at the foot of the guy wires south of meteorological mast 3, approximately 60 m from the mast (see **Figure 3**). The WC258 is an upgraded version with Flow Complexity Recognition (FCR). This FCR system uses a fifth vertical beam to measure the vertical wind speed, which enables a reduction of the measurement bias in complex terrain and complex flow [2]. However, since the test site EWTW is considered as fairly simple terrain, the effect of this fifth beam is expected to be insignificant for this study and therefore this algorithm is not considered.

Up to 10 different range gates can be measured simultaneously using the laser pulse time, allowing to measure the wind speed at 10 different heights. The WindCube has been configured to have three of these measurement heights identical to the measurement heights of the met mast (i.e. 52, 80 and 108 meter). Turbine geometry, measurement heights and relative distance (201m, i.e. 2.51 times the rotor diameter) are drawn to scale in **Figure 4**.

The data from the WC258 is available in the LAWINE database from 22-11-2012 until 23-01-2014.

Figure 4: Schematic showing distance to turbine, LiDAR cone angle and measurement heights of LiDAR and meteorological mast.



2.4 Wind turbine load measurements

The measurement campaign is performed on the ECN research turbine number N6. The research turbine has a 80m hub height and 80m rotor diameter. Rated power is 2.5MW. Loads are measured using strain gauge bridges as described in [2]. Measured and calculated load quantities are depicted in **Figure 5** and summarized in **Table 1**.

Figure 5: Schematic showing load measurement locations on N6 turbine.

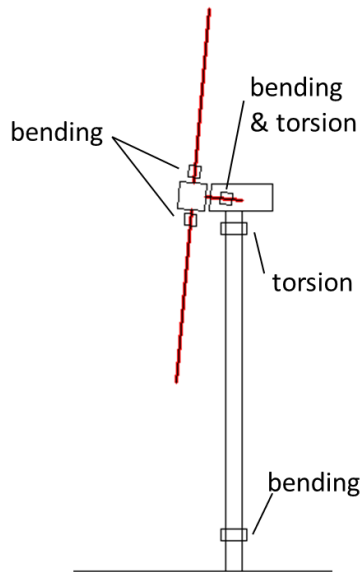


Table 1: Measured and calculated load quantities for N6 research turbine.

sensor position	location	bridge type	measured load quantities	calculated load quantities
blade root	1.33m from blade flange (blade 1, 2, 3)	full bridges (parallel gauges)	blade edge and flapwise bending	rotor in-plane moment, rotor out-of-plane moment
main shaft	middle between main bearing and shrink disk	full bridges (T-gauges resp. +45/-45 strain gauges)	shaft bending moment in rotating coordinate system; shaft torsion moment	shaft tilt moment; shaft yaw moment
tower top	1.61m below the tower top	full bridges (+45/-45 strain gauges)	tower torsion moment	
tower bottom	7.31m above foundation	full bridges (T-gauges)	bending moment in East-West and North-South direction	bending moment in tilt and roll direction

2.5 Measurement data

Simultaneous measurements of turbine, LiDAR and meteorological mast were collected for a period of 9 months (May 2013 to January 2014). A total of 2744 ten-minute samples (457 hours of data) is used after filtering for valid turbine, LiDAR, met mast and loads signals. Only samples from the undisturbed wind direction sector described in [2] are used.

Eight LiDAR heights are used for analysis of wind shear in Chapter 3: 40, 52, 80, 100, 108, 140, 160 and 200 m.

The distribution of wind speeds and turbulence intensities contained in the data set is summarized in the matrix in **Table 2**. As a measure of statistical representativeness of the data set the available amount of ten-minute samples is compared to the minimum required amount in a IEC61400-13 loads measurement campaign as shown in the table. In nearly all wind speed bins (highlighted in green) the number of samples exceeds the IEC requirement.

Table 2: Matrix showing number of ten-minute samples binned according to wind speed and turbulence intensity. Comparison with minimum required number of samples in IEC61400-13 is shown at bottom of table.

Total	V_bin [m/s]																									
Tl_bin [%]	<3.5	4	5	6	7	8	9	10	11	12	13	14	15	16	17	18	19	20	21	22	23	24	25	>25.5	Grand Total	
<3	0	17	39	81	35	14	6	0	0	0	0	0	0	0	0	0	0	0	0	0	0	0	0	0	0	192
4	0	36	47	54	48	47	5	3	0	0	1	0	0	0	0	0	0	0	0	0	0	0	0	0	0	241
6	0	19	37	44	54	45	21	23	8	1	2	1	1	0	0	0	0	0	0	0	0	0	0	0	0	256
8	0	20	37	40	74	78	72	61	30	19	12	11	8	5	2	2	2	2	0	0	1	0	0	0	0	474
10	0	14	42	48	80	73	98	92	52	29	19	22	22	6	14	11	5	3	4	1	1	0	0	0	0	636
12	0	16	43	51	56	47	62	85	51	31	12	7	15	6	6	13	2	0	2	2	0	0	0	0	0	507
14	2	14	26	29	24	40	37	30	25	9	6	5	2	0	1	2	0	2	0	0	0	0	0	0	0	254
16	0	7	15	23	16	13	14	17	6	2	2	0	1	0	0	0	0	0	0	0	0	0	0	0	0	116
18	0	4	7	5	4	3	4	5	1	0	1	0	0	0	0	1	0	0	0	0	0	0	0	0	0	35
20	0	2	4	2	0	1	2	2	2	0	0	1	0	0	0	0	0	0	0	0	0	0	0	0	0	16
22	0	1	1	0	1	1	0	0	1	0	0	0	0	0	0	0	0	0	0	0	0	0	0	0	0	5
24	0	0	0	0	0	0	0	1	1	0	0	0	0	0	1	0	0	0	0	0	0	0	0	0	0	3
26	0	0	0	1	0	0	0	0	0	0	0	0	0	0	0	0	0	0	0	0	0	0	0	0	0	1
28	0	0	0	0	0	0	0	1	1	0	0	0	0	0	0	0	0	0	0	0	0	0	0	0	0	2
>29	0	1	0	1	0	0	0	0	2	0	1	0	0	0	0	0	1	0	0	0	0	0	0	0	0	6
Grand Total	2	151	298	379	392	362	321	320	180	91	56	47	49	17	24	29	10	5	6	4	1	0	0	0	0	2744
required for IEC61400-13	0	30	30	30	30	30	30	30	30	30	30	30	30	8	8	8	8	8	8	1	1	1	1	1	1	0

3

Analysis of shear and loads

3.1 Introduction

In this chapter first the vertical wind shear of the ten-minute samples in the measured data set is analysed.

Vertical wind shear is determined using the power law and shear exponent α .

Next the effect of wind shear on turbine loads is investigated using the loads measurement on the N6 turbine. The following load components that are measured during the campaign are assumed to be influenced by vertical wind shear and will be analysed:

- Blade out-of-plane fatigue moment
- Static main shaft tilt moment
- Dynamic main shaft bending moment
- Tower base fore-aft fatigue bending moment

3.2 Analysis of wind shear in measurement data

Vertical wind shear is described by the power law:

$$U(z) = U_{ref} * (z/z_{ref})^{\alpha}$$

where

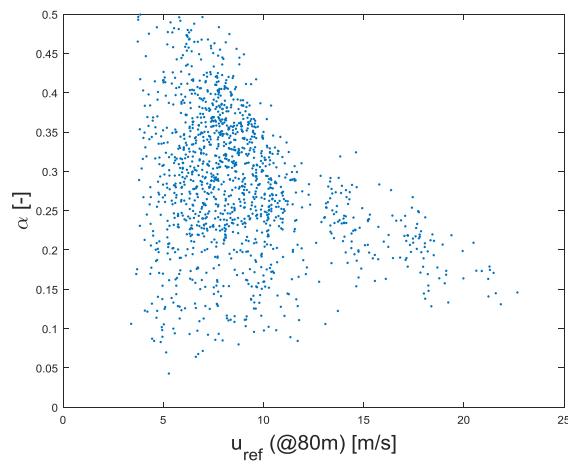
- $U(z)$ is the wind speed at height z ,
- U_{ref} is the wind speed at reference height
- z_{ref} is the reference height
- α is the wind shear (or power law) exponent

The turbine hub height (80m) is used as reference height. For each ten-minute sample in the data set the shear exponent α is determined by means of linear regression using the eight LiDAR measurement heights. A secondary result of the regression is the reference speed (U_{ref}); this is the wind speed on the fitted wind speed profile at the reference height.

Analysis of the shear characteristics of the available measurement data is described in detail in **Appendix A**. Data samples with a poor regression fit for α ($R^2 < 0.97$) are filtered out, causing 51% rejection of data. The resulting distribution of shear exponents versus wind speed is shown in **Figure 6**. In the remainder of this report the following filters are applied:

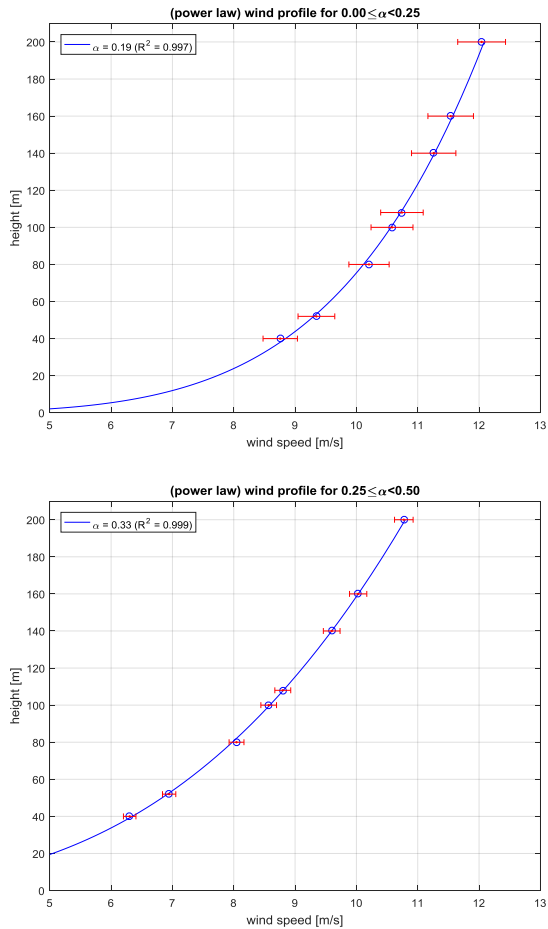
- alpha values are limited to the range from 0 to 0.5.
- turbulence intensity (derived from meteorological mast wind speed at 80m) range of 0 - 20%, to remove a few outliers.

Figure 6: Distribution of shear exponent α versus reference wind speed U_{ref} .



To visualize the general shear profile of the data the samples are divided in two α -ranges and the resulting average wind profiles are shown in **Figure 7**.

Figure 7: Average wind shear profile for two α -bins.



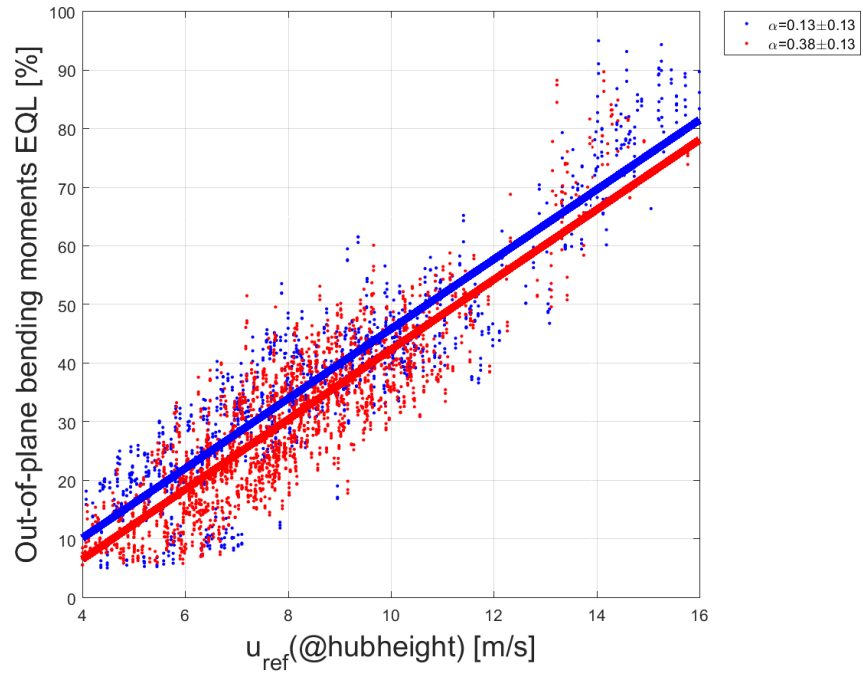
3.3 Effect of shear on Blade Out-of-plane Fatigue Moment

The primary load component that is expected to see the effect of shear is the blade fatigue load in the direction perpendicular to the rotor surface. This load is assumed to be heavily affected by the shear profile while the blades rotate through the incoming wind field. It is assumed that a higher α results in a higher fatigue load.

Figure 8 below shows the fatigue equivalent out-of-plane root bending moment (M_{Op} EQL) versus wind speed (U_{ref}) for two wind shear parameter alpha bins including regression lines. Contrary to the assumption a higher shear results in a lower blade out-of-plane fatigue moment. For this reason turbulence intensity is considered next and it is evaluated if turbulence intensity has a dominating effect on the M_{Op} EQL compared to wind shear. It is noted that Figure 8 contains samples with a TI of 0 to 20 %. The fatigue

equivalent out-of-plane root bending moment in **Figure 8** is shown as percentage, normalized to the full range of the contained samples.

Figure 8: Blade Out-of-plane Fatigue Moment (normalized) vs. reference wind speed for two alfa bins.



The distribution of wind shear parameter alpha vs. Turbulence Intensity for the samples is shown below.

Figure 9: Dependence between wind shear and turbulence intensity.

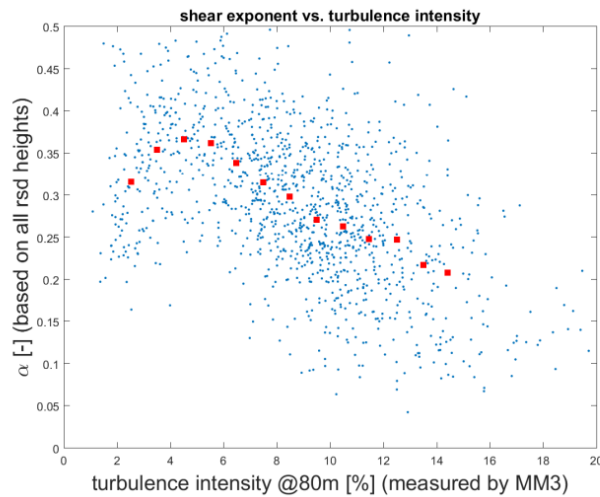
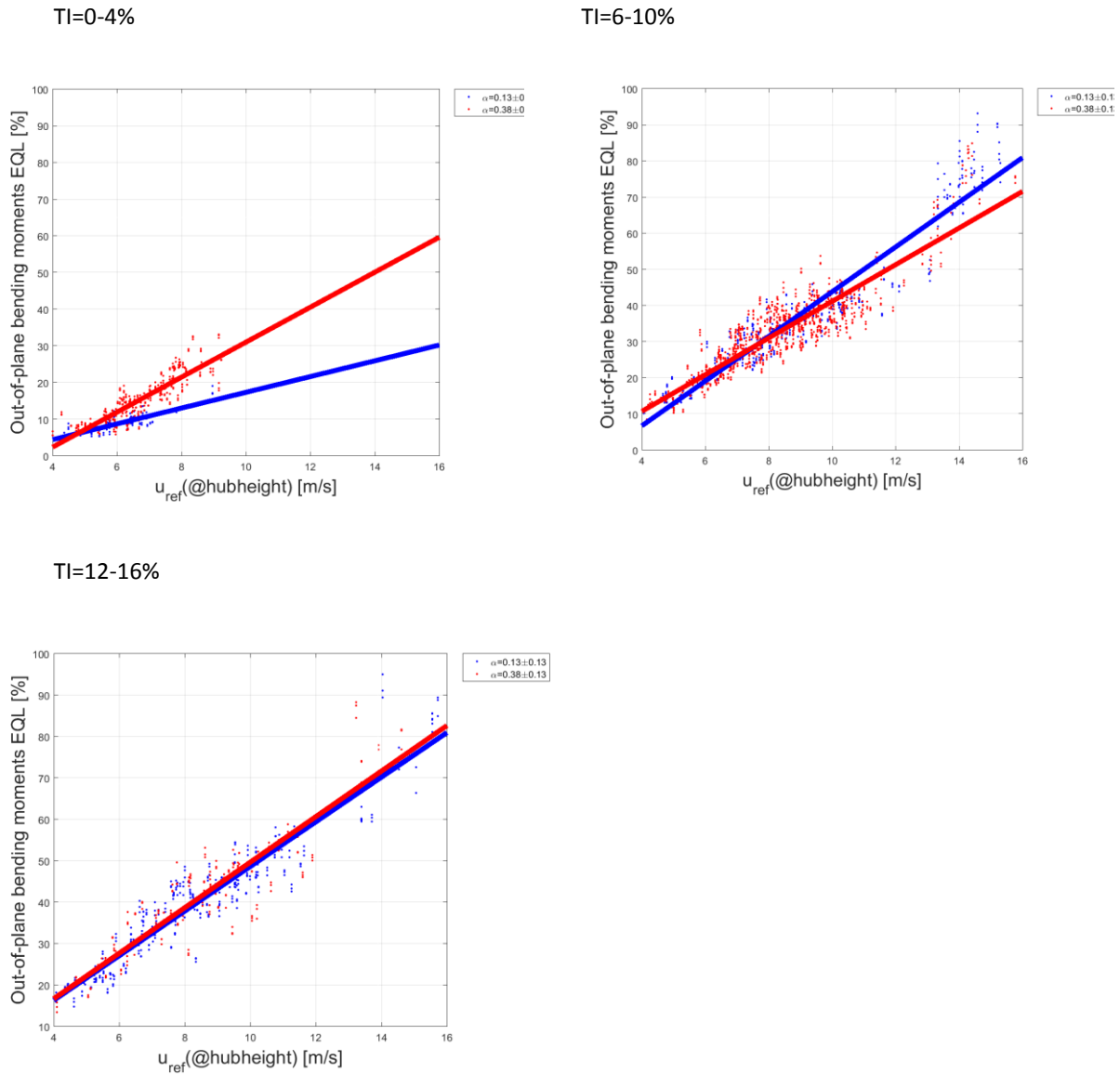


Figure 9 clearly demonstrates that the lower alpha bin (0-0.25) correlates with relatively high turbulence intensity levels. This is considered to be an effect of atmospheric stability: in case of higher turbulence, more mixing between atmospheric layers takes

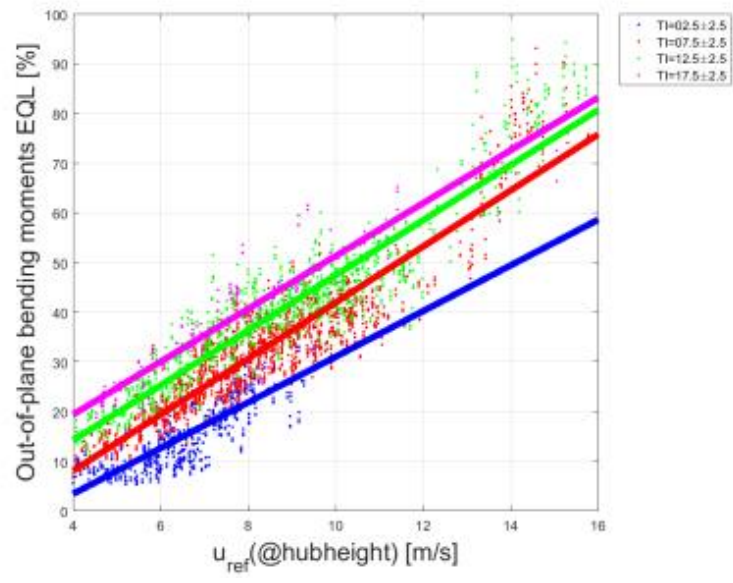
place and shear will be lower than with lower turbulence (see also [3]). It appears that the blade out-of-plane fatigue moment is dominated by TI, rather than alpha. This effect of TI is visualized by limiting the TI range of samples included in the plot. In **Figure 10** the blade out-of-plane fatigue moment is shown for three TI ranges between 0 and 16%.

Figure 10: Blade M_{OP} EQL (normalized) for two α -bins at three different TI ranges.



For low turbulence intensity (0-4%) the assumption holds and the blade out-of-plane fatigue moment increases with higher alpha. For higher turbulence intensity level (6-10% and 12-16%) alpha does not affect the fatigue moment. The dominant effect of turbulence intensity on the fatigue moment is confirmed when plotting M_{OP} EQL versus U_{ref} for binned TI as shown in **Figure 11**. This is in line with observations from load simulations reported in [4]. Comparing an increase from 2.5% turbulence intensity bin to the 17.5% bin, the M_{OP} EQL increases app. 15%.

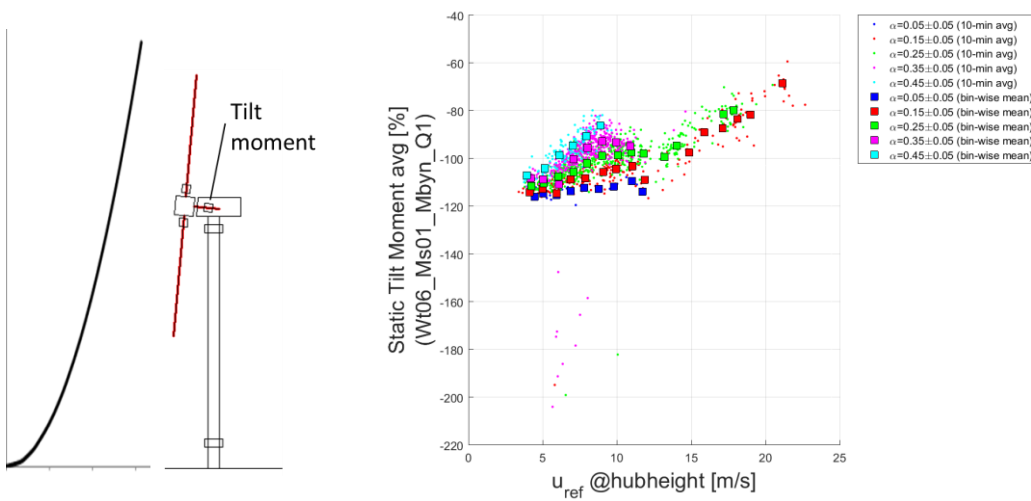
Figure 11: Blade Out-of-plane Fatigue Moment (normalized) vs. reference wind speed for five TI bins.



3.4 Effect of shear on Static Main shaft tilt moment

The effect of the measured shear exponent α on the average static main shaft tilt moment (10-minute average value in fixed coordinate system) is analysed. The result is shown in the **Figure 12**. This bending moment in this plot (and subsequent plots) is plotted as percentage of the average from the plotted data. A clear dependence on α is observed: the higher the α , the higher the average static main shaft tilt moment. The maximum difference (α -bin 0.05 compared with α -bin 0.45) is 30% and occurs at 8m/s.

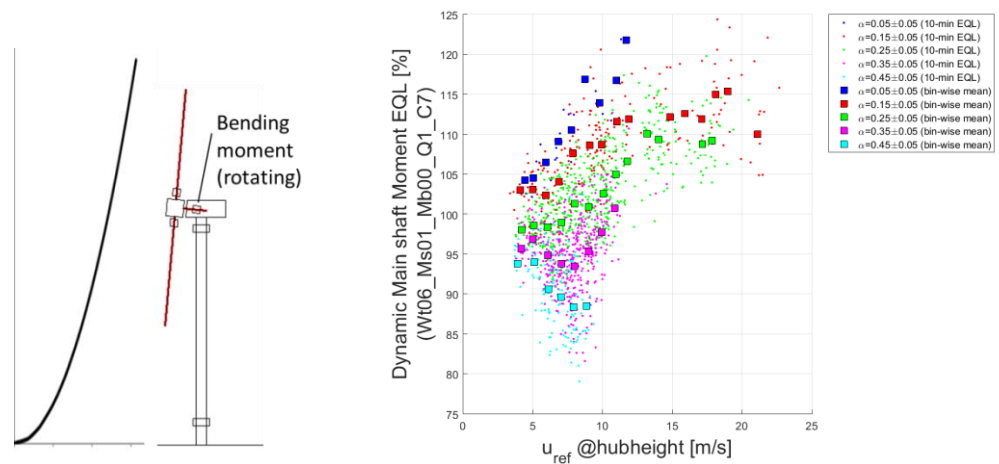
Figure 12: Average static main shaft tilt moment (normalized) and effect of shear.



3.5 Effect of shear on Dynamic Main shaft fatigue bending moment

The effect of the measured shear exponent α on the dynamic main shaft fatigue equivalent bending moment (bending of main shaft in rotating coordinate system) is analysed. The result is shown in **Figure 13**. A dependence on α is observed: the higher the α , the lower the fatigue bending moment of the rotating shaft. This is in line with the observation in paragraph 3.3 and **Figure 8** for the blade M_{OP} EQL. The lower TI for the samples with higher α results in a lower main shaft fatigue bending moment.

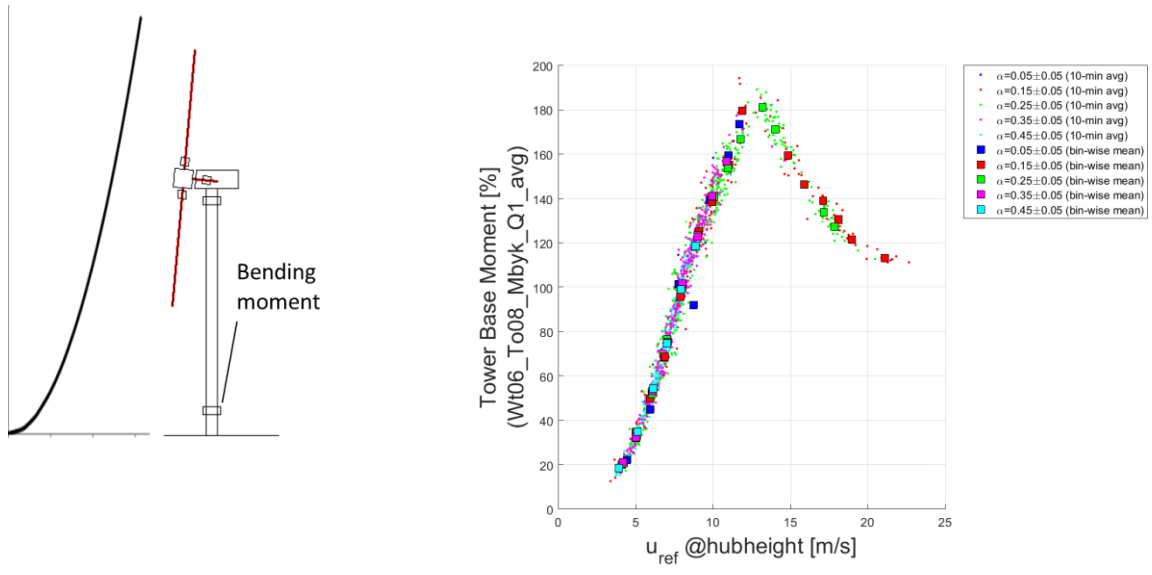
Figure 13: Dynamic Main shaft fatigue bending moment (normalized) and effect of shear.



3.6 Effect of shear on Static Tower base for-aft bending moment

The effect of the measured shear exponent α on the average static tower base for-aft bending moment (10-minute average value) is analysed. The result is shown in **Figure 15**. No dependence on α can be observed. Although the average static main shaft tilt moment (paragraph 3.4) showed a dependence on the wind profile (α), the average tower base bending moment is seen not to be influenced by the wind profile but dominated by the moment from thrust force times hub height.

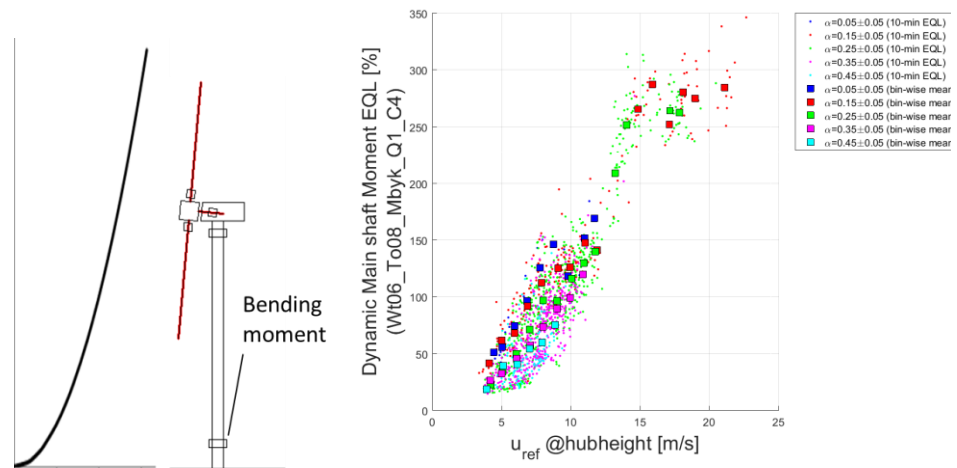
Figure 14: Tower base for-aft average static bending moment (normalized) and effect of shear.



3.7 Effect of shear on Tower base for-aft fatigue bending moment

The effect of the measured shear exponent α on the tower base for-aft fatigue equivalent bending moment is analysed. The result is shown in **Figure 15**. Unlike for the average tower base bending moment (paragraph 3.6) a dependence on α is observed: the higher the α , the lower the fatigue bending moment of the tower base. This result (the effect of lower TI at higher α) is comparable to the observations for the blade M_{OP} EQL (paragraph 3.3).

Figure 15: Tower base for-aft fatigue bending moment (normalized) and effect of shear.



4

Conclusions & Recommendations

LiDAR measurements and turbine loads measurements for blades, main shaft and tower base were analysed for the N6 research turbine. Shear exponent α in the dataset was found to be inversely correlated to turbulence intensity.

The assumption that blade out-of-plane bending moment increases with higher shear was investigated.

- For low TI (0 to 4%) a dependence between blade out-of-plane EQL and α is confirmed. Blade fatigue load increases with shear at low turbulence.
- For higher TI values (6 to 20 %) the effect of turbulence dominates the blade out-of-plane fatigue load and no effect of α is observed. An increase from 2.5% to 17.5% turbulence intensity showed a maximum of 15% higher out-of-plane EQL.

Main shaft average non-rotating bending moment was observed to increase with higher shear (i.e. up to 30% increase was observed). Fatigue equivalent bending moment of the main shaft in rotating coordinate system reduces with higher α (lower TI), in line with blade out-of-plane EQL.

Average static tower base for-aft bending moment was observed to be independent from shear and is expected to be dominated by rotor thrust. Tower base for-aft fatigue equivalent bending moment however decreased with higher α (lower TI), again similar to blade out-of-plane EQL.

Investigation of further correlations between LiDAR measurements and wind turbine loads are recommended:

- Effect of TI distribution (versus height) on turbine loads
- Effect of wind veer distribution (versus height) on turbine loads
- Other shear categorization instead of power law
- Investigate influence of wind upflow angle
- Comparison with mechanical load simulations

LiDAR measurements are shown to provide solid information on shear that is strongly correlated to loads on main wind turbine components: blades, main shaft and tower. Compared to traditional meteorological masts, LiDAR provides a low-cost opportunity to measure wind speed at multiple heights and enable a refined determination of turbine loads. This can be applied in the following areas:

1. Resource assessment phase

LiDAR measurements during resource assessment phase can be used to classify shear levels that occur at a site, enabling better accuracy in site-specific loads assessments.

2. Operational phase

LiDAR measurements and determination of shear and turbulence levels in the operational phase of a wind farm can be used for improved monitoring of actual static and fatigue loads. This is useful for optimization of maintenance and prediction of remaining life time.



References

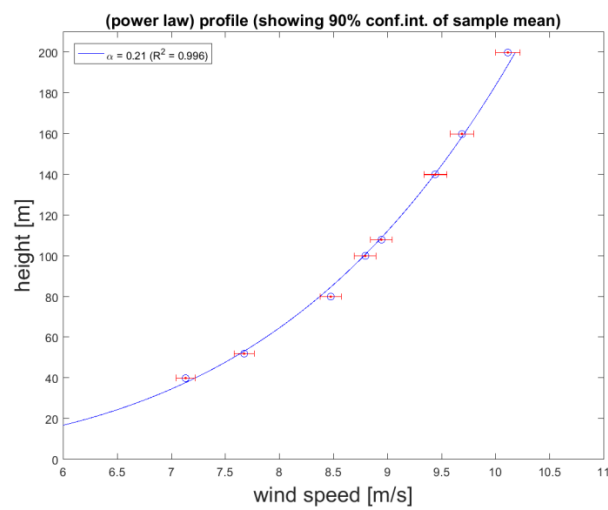
- [1] Measurement Plan LAWINE project tasks A and C, ECN-X--13-059, November 2013, J.W. Wagenaar, G. Bergman, K. Boorsma
- [2] LAWINE instrumentation report, ECN-X--14-085, June 2014, G. Bergman, J.W. Wagenaar, K. Boorsma
- [3] Model of wind shear conditional on turbulence and its impact on wind turbine loads, N. Dimitrov et al., DTU, 2014
- [4] Influence of atmospheric stability on wind turbine loads, A. Sathe, J. Mann, DTU and TUD, 2012
- [5] IEC61400-12-1-CDV (E), Wind Turbine Generator Systems - Part 12-1: Wind Turbine Power Performance Testing, 2016-5.

Appendix A. Analysis of shear data

In this appendix the available measurement data is analysed in detail in order to gain more insight in the shear characteristics.

First the campaign-averaged shear using the eight measurement heights is determined: mean $\alpha = 0.21$. See figure below.

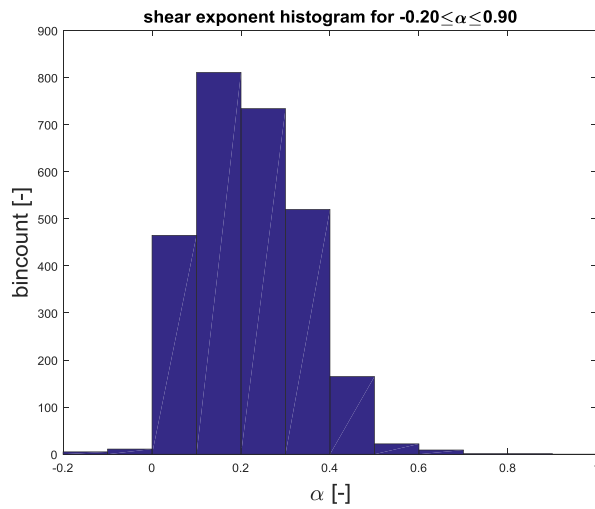
Figure 16: campaign-averaged shear.



This proves that on average using all 8 available LiDAR heights is a good representation for the shear across the rotor plane.

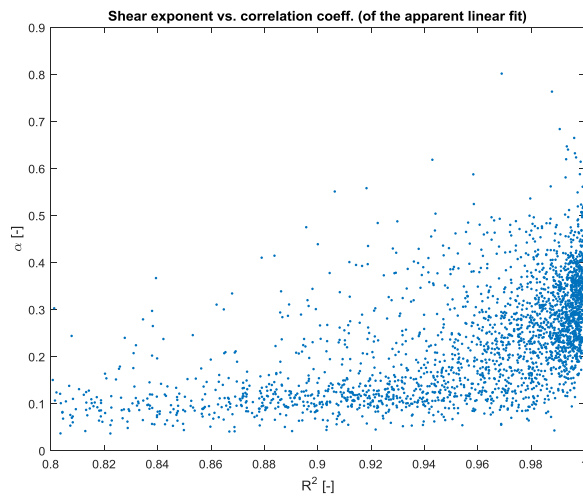
Next α is determined for each 10-minute sample. The distribution of binned α values, between -0.2 and 0.9, is shown in **Figure 17**.

Figure 17: Histogram of alfa in data set.



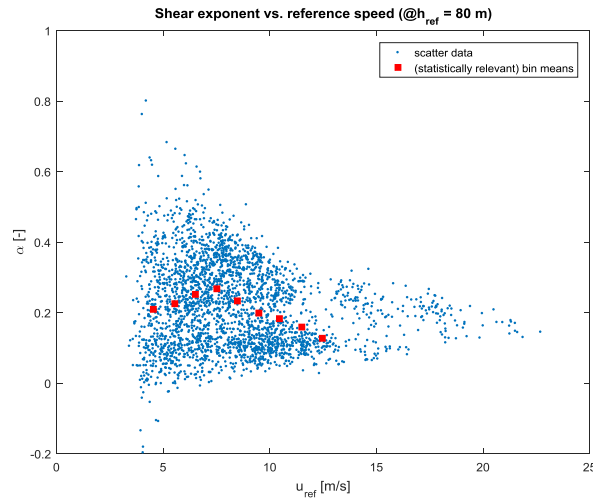
The strength of the alfa regression fit for the data samples, expressed by the coefficient of determination R^2 , is shown in **Figure 18**

Figure 18: Strength of the alfa regression fit in data set



The scatter of alfa samples over reference wind speed is shown in **Figure 19**, including bin means. Here the statistical relevance of the bin means is determined by: $\text{bincount} > \text{total number of samples} / (2 * \text{the number of bins})$.

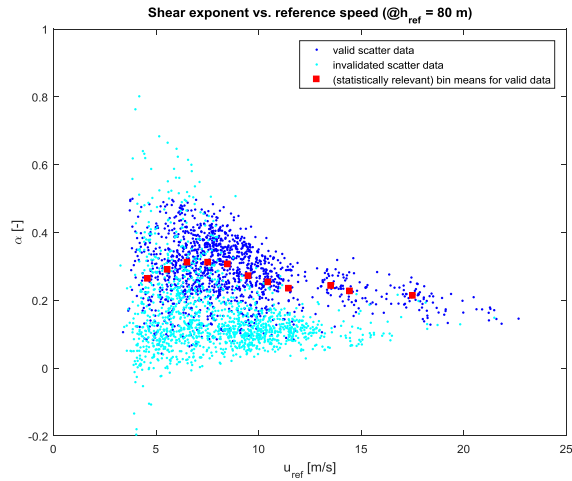
Figure 19: Shear exponent vs. reference wind speed



To avoid using samples that have a poor fit to the power law a minimum R^2 level is set. The chosen level is $R^2 > 0.97$ (equal to the minimum R^2 for LiDAR validation KPIs by CT-OWA). This results in a rejection rate of 51%. Furthermore the samples are filtered for an alpha range of 0 to 0.5.

The remaining and rejected samples are shown in **Figure 20**. Most rejected samples (with low R^2) are observed to have a low alpha (in the range of 0 – 0.2).

Figure 20: Sample rejection ratio vs. the acceptance level of R^2 .



Furthermore for the loads analysis in this report the following wind speed and turbulence ranges are used:

- U_{ref} wind speed range of 4-16 m/s
- turbulence intensity (derived from meteorological mast wind speed at 80m) range of 0 - 20%



ECN

Westerduinweg 3
1755 LE Petten
The Netherlands

P.O. Box 1
1755 LG Petten
The Netherlands

T +31 88 515 4949
F +31 88 515 8338
info@ecn.nl
www.ecn.nl

